Available online at www.sciencedirect.com
SCIENCE DIRECT
Journal of Catalysis 233 (2005) 166–175
JOURNAL OF CATALYSIS
www.elsevier.com/locate/jcat

Role of sulphates on the mechanism of NH_3-SCR of NO at low temperatures over presulphated vanadium supported on carbon-coated monoliths

E. García-Bordejé [a,*], J.L. Pinilla [a], M.J. Lázaro [a], R. Moliner [a], J.L.G. Fierro [b]

[a] *Instituto de Carboquímica, CSIC, Miguel Luesma Castán 4, 50015 Zaragoza, Spain*
[b] *Instituto de Catálisis y Petroleoquímica, CSIC, Marie Curie s/n, Cantoblanco, 28049 Madrid, Spain*

Received 7 March 2005; revised 15 April 2005; accepted 21 April 2005
Available online 25 May 2005

Abstract

A novel catalyst was prepared by sulphation of vanadium supported on carbon-coated monoliths with a mixture of $SO_2 + O_2$ at 473 K. The as-sulphated catalyst shows about twofold higher conversion than the fresh catalyst in the selective catalytic reduction of NO at low temperatures (<473 K) after an induction period. The increase in activity during the induction period is correlated with the buildup of more stable sulphate species. The sulphated catalyst was characterised by temperature-programmed desorption, photoelectron spectroscopy, temperature-programmed reaction, and transient response techniques. We have found evidence indicating that sulphates are anchored to carbon in the vicinity of vanadyl sites. This fact can account for the improvement of the redox properties in the sulphated catalyst. On the basis of experimental results, the enhancement of the redox properties, rather than the increase in acidity, is the cause of the superior performance of the sulphated catalyst compared with the fresh one.

Keywords: Vanadium oxide catalyst; Carbon-coated monoliths; SCR of NO; Sulphated catalyst

1. Introduction

In the selective catalytic reduction (SCR) of NO by ammonia, the optimum operating temperature of the commercial catalyst (i.e., V_2O_5/TiO_2 promoted with WO_3 or MoO_3) is in the range of 573–673 K, which makes it necessary to reheat the flue gas after the electrostatic precipitator and desulphuriser (393–523 K). In an effort to avoid reheating costs, the search for new catalysts that are active and stable at low temperatures is still under way. In recent years, a considerable effort has been devoted to developing a catalyst that is active at low temperatures. Some examples are MnO_x/Al_2O_3 [1], MnO_x/TiO_2 [2], MnO_x/NaY zeolite [3], V_2O_5/activated carbon [4,5], MnO_x/activated carbon [6,7], and unsupported Fe–Mn [8].

Commercial SCR catalyst contains about 0.5–1% sulphur, which is present mainly in the form of sulphate on the surface. Some authors have suggested that surface sulphates have a promoting effect in the SCR of NO at high temperatures [9–14]. All of these authors agree that this promotion occurs because NH_3 adsorption is enhanced by the increase in acidity by surface sulphates. Upon sulphation of the support, the acid sites increase in both number and strength. The latter is due to the inductive effect of the S=O bond [9,12]. Lietti et al. [11] suggested that NH_3 adsorbs to the surface of S sites acting as an ammonia reservoir. Amiridis et al. [15] have also found a promoting effect when SO_2 is present in the feed for VO_x/TiO_2 loading below half a monolayer, and it was argued that sulphates favour the polymerisation of vanadyl species. In SCR at low temperatures with V_2O_5/activated carbon [5,16,17], an increase in the activity was observed when SO_2 was present in the feed. These

* Corresponding author. Fax: +34 976733318.
E-mail address: jegarcia@carbon.icb.csic.es (E. García-Bordejé).

0021-9517/$ – see front matter
doi:10.1016/j.jcat.2005.04.032

authors proposed that the increase in activity is due to the formation of $SO_4^=$ linked to carbon, which increases acid sites that adsorb NH_3.

The mechanism of reaction and the nature of sulphated species have been exhaustively studied in SCR at high temperatures over sulphated oxidic supports. However, the literature dealing with NH_3-SCR at low temperatures over sulphated carbon-supported catalyst is very scarce, and the mechanism of promotion by sulphates is still not well understood. In the literature, the promoting effect of sulphates is usually attributed to an increase in acid sites, neglecting other factors, such as the influence of sulphates on redox properties or electronic effects. We have shown previously [18] that a presulphated vanadium catalyst on carbon-coated monolith exhibits activity superior to that of the sulphur-free catalyst. In this work, we present the results of a comprehensive study of the mechanism of NH_3-SCR over sulphated catalyst. The use of transient response techniques, temperature-programmed techniques (TPR, TPD), and XPS has enabled us to shed some light on the reasons for the higher activity of the sulphated catalyst compared with the fresh one.

2. Experimental

2.1. Catalyst preparation

Cordierite monoliths (400 cpsi, 1-cm diameter, 5-cm length) were coated with a polymer blend by a method described elsewhere [19]. The polymers used were furan resin (Huttenes–Albertus) and polyethylene glycol-6.000 MW (Sigma-Aldrich). After thermal curing, the monoliths were carbonised at 973 K, activated with CO_2 at 1173 K for 4 h (30% carbon burn-off), and treated for 18 h with 2 N HNO_3 at room temperature to develop oxygenated surface groups.

The as-prepared carbon-coated monoliths (CCM) were loaded with 5 wt% vanadium. The impregnation was carried out by ion exchange with a solution of ammonium metavanadate in a stoichiometric amount to get a 5 wt% V-loading. To facilitate the dilution of ammonium metavanadate, ca. 10 mg of oxalic acid was added. Under these conditions the pH of the solution remained neutral, and the solution had a yellow colour, which was indicative of the presence of VO_2^+.

The monoliths, placed in a holder, were introduced into a vessel with 100 ml of the impregnating solution. The vessel had a stirrer at the bottom that created a continuous flux of the vanadium solution through the monolith channels. This guaranteed that vanadium is deposited uniformly inside the channels. This process was allowed to proceed for 18 h. Subsequently, the monoliths were rinsed thoroughly with distilled water in the same setup. Thus it was ensured that only vanadium strongly adsorbed to the support remained in the pores. After the monoliths were dried first at room temperature overnight and later 2 h at 383 K, the catalyst was calcined in Ar at 673 K. The vanadium content of the resulting catalysts was analysed by inductive coupled plasma-optical emission spectroscopy (ICP-OES).

To prepare the presulphated catalyst, we sulphated 5 wt% vanadium on carbon-coated monoliths by passing 50 ml/min of 400 ppm SO_2, 3% O_2, and Ar (balance) at 473 K over the vanadium on CCM catalysts for 18 h.

2.2. Characterisation of catalysts

The sulphate species in the presulphated catalyst after several stages of the SCR reaction was characterised by temperature-programmed desorption (TPD). PRE-SCR stands for the sulphated catalyst previous to SCR reaction, and the catalyst samples after reaction are denoted by SCR followed by the reaction time in minutes. TPD experiments were carried out in a quartz microreactor. In a typical experiment, 50 ml/min of Ar was passed over the catalyst until the signal of the mass spectrometer was stable. Later the temperature was raised to 773 K at a rate of 10 K/min. The desorptions of NH_3 and SO_2 were followed by m/e 17 and 64, respectively, in the mass spectrometer. The desorption profile of SO_2 was fitted to three peaks that coincided with desorption temperatures similar to those described in the literature [20]. We estimated the areas of these peaks by calculating the integral of each peak after subtracting the baseline and fitting the experimental peaks to Gaussian lines of variable width.

Temperature-programmed desorption of preadsorbed ammonia (NH_3-TPD) was also carried out as described above. The only differences were that the catalyst was pretreated with 50 ml/min of 1800 ppm NH_3 in Ar for 2 h at 373 K, and the temperature was raised to 1073 K.

X-ray photoelectron spectroscopy (XPS) was used to study the chemical composition of the catalyst surface. Photoelectron spectra were recorded with a VG Escalab 200R electron spectrometer equipped with a Mg-Kα X-ray source ($h\nu = 1253.6$ eV) and a hemispherical electron analyser operating at a constant pass energy (50 eV). The C 1s peak at 284.9 eV was used as an internal standard for peak position measurements.

2.3. Catalytic tests

The catalytic tests were performed in a 14-mm i.d. quartz microreactor. We forced the gas to flow through the monolith channels by fixing the monoliths to the inner walls of the reactor with teflon stripe. The total amount of carbon coating was ca. 0.12 g, and the total flow rate was 100 ml/min STP, which yields a GHSV of $\sim 34{,}000\ h^{-1}$. Catalytic tests were carried out with 5 wt% V catalyst, both fresh and after the presulphation process. The gas composition used was 500 ppm NO, 600 ppm NH_3, and 3% O_2, and the balance was Ar. First, the reaction temperature was set at 393 K and

the reaction was allowed to proceed for 2 h until steady-state was reached. Subsequently, the temperature was raised to 423 K, and the same process was repeated with 438, 453, 473, 493, and 523 K up to stationary conversion. In all of the experiments the amounts of N_2O were less than 5 ppm, and no oxidation of ammonia took place, as determined by nitrogen balance.

A mass spectrometer (Balzers) was used to analyse the gas stream. The zero was measured before every experiment to correct possible variations with the time. Mass spectrometer signals were calibrated with cylinders of gases with certified known composition. The following main mass-to-charge (m/e) ratios were used to monitor the concentration of products and reactants: 17 (NH_3), 18 (H_2O), 28 (N_2), 30 (NO), 32 (O_2), 44 (N_2O), and 46 (NO_2). The fragmentation pattern of each gas was dealt with as follows. From the mass m/e 12 and taking into account that the contribution of CO_2 to m/e 12 is 6%, the amount of CO_2 desorbed at steady state was calculated. The N_2O concentration was calculated from m/e 44 after the contribution of CO_2 was subtracted. The NO concentration was calculated from m/e 30, after the contribution to this mass of N_2O (30%) was subtracted. The concentration of N_2 was calculated from m/e 28 after the contributions of N_2O (11%) and CO_2 (11%) were subtracted. Finally, the NH_3 concentration was obtained from m/e 17.

Transient-response experiments have been widely used to study the SCR of NO over V_2O_5–WO_3/TiO_2 catalysts [11,21,22]. We carried out experiments at 423 and 473 K with stepwise addition-removal of one of the reactants, either NH_3 or NO. Contrarily to steady-state experiments, the dynamics of SCR reaction can be analysed. Thus these experiments allow unravelling of the steps involved in the mechanism of reaction. In the experiment with stepwise addition-removal of NO, the catalyst was previously saturated with 600 ppm NH_3 + 3% O_2 at the temperature of reaction, and in the experiment with stepwise addition-removal of NH_3 the catalyst was previously saturated with 500 ppm NO + 3% O_2.

Temperature-programmed reaction experiments were conducted in the presence of gas-phase oxygen (TPReaction) and in its absence. Because of their non-steady-state nature, TPReaction experiments are very useful for the study of the role of the catalyst functions on the SCR reaction. The experimental procedure was as follows. To saturate the surface with NH_3, 100 ml/min of a gas containing NH_3 (1700 ppm) was allowed to flow over the catalyst at 323 K for 1 h. Later, the gas was switched to Ar, and this was maintained for 30 min to remove weakly adsorbed NH_3. Subsequently, the reaction gas was admitted (i.e., 500 ppm NO, 600 ppm NH_3, 3% O_2, and balance Ar). In the TPReaction in the absence of O_2 the same composition was used, but without O_2. The temperature was raised to 523 K with a ramp of 5 K/min.

3. Results

3.1. Process of catalyst sulphation

It is widely reported that vanadium in oxidation state +5 undergoes a redox cycle and oxidises SO_2 to SO_3 [15, 23–25]. The oxidation of SO_2 over 5 wt% V/CCM was performed at three different temperatures, 433, 453, and 473 K. Gas containing 400 ppm SO_2, 3% O_2, and Ar (balance) was allowed to flow (50 ml/min) over 5 wt% V/CCM catalyst for 18 h. The SO_2 concentration at the outlet was monitored by mass spectrometry. This SO_2 concentration describes a typical breakthrough curve. The area over the curve was integrated, and thus the moles of converted SO_2 were quantified. The SO_2 thus calculated coincided, within less than 5% error, with the moles of sulphur determined by elemental analysis after the sulphation process, indicating that all SO_2 converted to SO_3 is retained by the catalyst-adsorbent. Fig. 1 plots the ratio of moles of adsorbed SO_2 to moles of vanadium as a function of reaction time. After 18 h the catalyst reached saturation regardless of the temperature. At saturation the ratio moles SO_2 moles/moles vanadium is higher than unity, that is, 1.4 at 453 and 473 K and 1.2 at 433 K. Values higher than 1 indicate that carbon support is involved in the adsorption of SO_3. The increase in this ratio from 433 to 453 K can be explained by the fact that the number of carbon sites accessible for adsorbing SO_3 increases with the temperature. This number of accessible carbon sites depends on the mean free path of surface diffusion of chemisorbed SO_3, which has a high activation energy [26].

3.2. Steady-state catalytic tests

Fig. 2 shows the NO conversion along with the CO_2 released at steady state as a function of the reaction temperature. It can be observed that the conversion is almost twofold higher in the presulphated catalyst than in the fresh one. The CO_2 signal takes longer to stabilise than the SCR

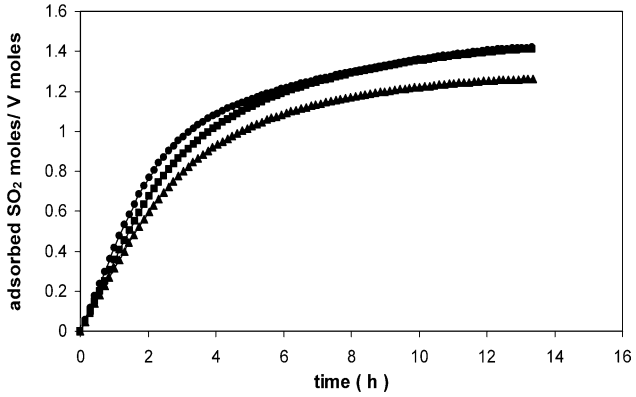

Fig. 1. Ratio of SO_2 moles to vanadium moles as a function of reaction time during presulphation of 5 wt% vanadium on carbon coated monoliths at three different temperatures: (▲) 433, (■) 453, and (●) 473 K. Reacting gas composition: 400 ppm SO_2, 3% O_2 and Ar to balance.

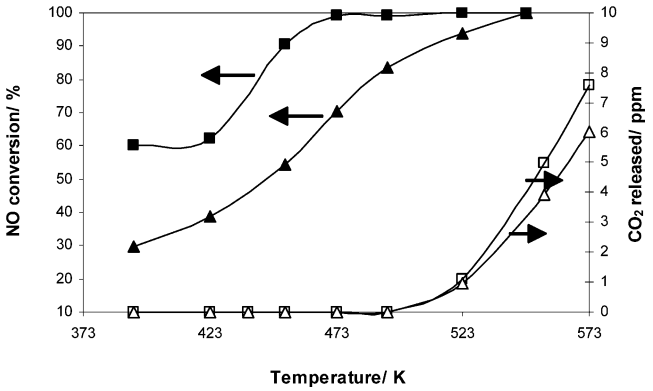

Fig. 2. NO conversion and CO_2 released in experiments at steady state as a function of the reaction temperature with fresh and presulphated catalyst containing 5 wt% vanadium: (▲, △) fresh catalyst, (■, □) presulphated catalyst; filled symbols = NO conversion, open symbols = CO_2 released. Reaction conditions: 0.1 g catalyst, [NO] = 500 ppm, [NH_3] = 600 ppm, 3% O_2, Ar to balance, total flow rate = 100 ml/min and GHSV = 34,000 h^{-1}.

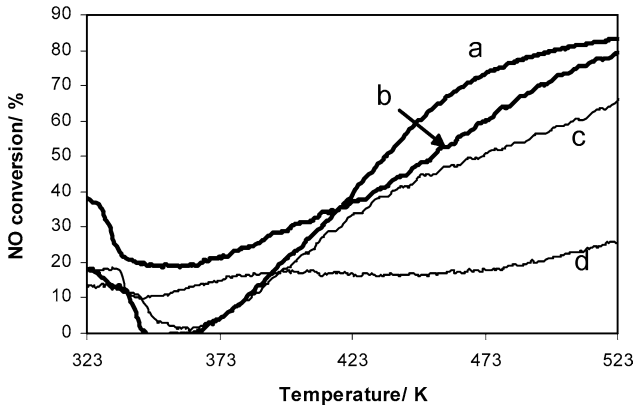

Fig. 3. Comparison of NO conversion in temperature-programmed reaction experiments in the presence of gas phase O_2 (TPReaction) and in its absence with the fresh and presulphated catalyst: curve (a) sulphated catalyst in the presence of 3% O_2, curve (b) fresh catalyst in the presence of 3% O_2, curve (c) sulphated catalyst in the absence of gas phase O_2, curve (d) fresh catalyst in the absence of gas phase O_2.

reaction (viz. around 6 h and 90 min, respectively) because the desorption of labile carbon groups is a slow process. No evolution of CO_2 at steady state occurs in the fresh or sulphated catalyst at temperatures lower than 500 K. This also shows that the role of sulphates catalysing the gasification of support is irrelevant. Since this catalyst is intended to be fitted in a tail end configuration, that is, downstream from the electrostatic precipitator and desulphuriser, the inlet temperature to the SCR unit will be lower than 500 K, and hence the gasification of support is not a matter of concern.

3.3. Temperature-programmed reaction techniques

Fig. 3 compares the NO conversion in temperature-programmed reaction experiments in the presence of 3% O_2 (TPReaction) and in the absence of O_2 in gas phase, with both the fresh and sulphated catalyst. In the sulphated catalyst, the conversion in the TPReaction experiment is considerably lower than it is under steady-state conditions (Fig. 2), because in the steady-state experiments an induction period was observed at all temperatures before the steady-state conversion was reached. At temperatures lower than 400 K, it is apparent that NO conversion is higher in fresh catalyst than in the sulphated one. This can be tentatively explained because NO is adsorbed on carbon basic sites of fresh catalyst. In contrast, basic sites of carbon are not available in the sulphated catalyst because they have previously been occupied by sulphates.

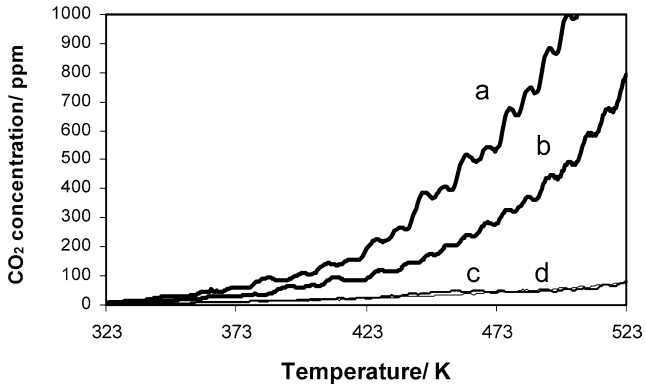

Fig. 4. CO_2 released in temperature-programmed reaction experiments in the presence of gas phase O_2 (TPReaction) and in its absence with the fresh and presulphated catalyst: curve (a) sulphated catalyst in the presence of 3% O_2, curve (b) fresh catalyst in the presence of 3% O_2, curve (c) sulphated catalyst in the absence of gas phase O_2, curve (d) fresh catalyst in the absence of gas phase O_2.

In TPReaction in the absence of O_2 over fresh catalyst (curve d), after a slight increase in conversion up to 373 K, the reaction is not able to proceed further. In sulphated catalyst, the curves of TPReaction (curve a) and TPReaction in the absence of O_2 (curve c) are comparable up to ca. 400 K. Above this temperature, the curve of TPReaction in absence of O_2 is slightly under the curve of TPReaction in the presence of 3% O_2. However, in contrast to the fresh catalyst, the reaction proceeds to a significant extent in the absence of O_2 in gas phase. The superior redox properties of the sulphated catalyst must stem from the fact that V^{4+} can be readily reoxidised to V^{5+} by lattice oxygen coming from surface sulphate species. It is worth noting that there is no SO_2 desorption in these experiments; therefore sulphates are not desorbed from the carbon surface.

To assess the effect of this lattice oxygen on the gasification of the most labile carbon groups of support, Fig. 4 shows the CO_2 evolution in TPReaction and TPReaction in the absence of O_2 with fresh and sulphated catalyst. The amount of evolved CO_2 in TPReaction experiments is slightly higher for the sulphated catalyst (curve a) than for the fresh one (curve b). The CO_2 release occurs at lower temperatures in TPReaction experiments than at steady state (Fig. 2), because at the beginning of the reaction the more labile or reactive carbon groups are gasified, and, subsequently, CO_2 desorption declines slowly with time on stream up to the sta-

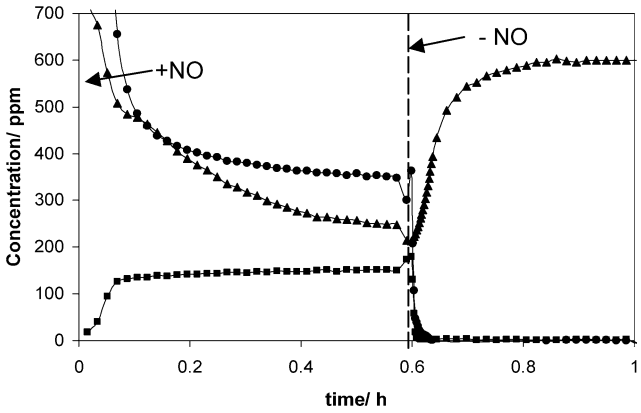

Fig. 5. Concentration of reactants upon stepwise addition-removal of NO in the SCR of NO at 473 K with 5 wt% vanadium fresh catalyst: (▲) NH_3, (■) NO, (●) N_2. Reacting gas composition: [NH_3] = 600 ppm, 3% O_2, [NO] = 500 ppm (when added), Ar to balance, total flow rate = 100 ml/min and GHSV = 34,000 h^{-1}.

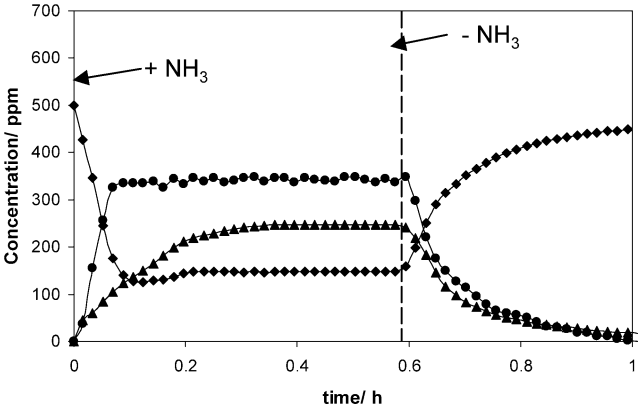

Fig. 6. Concentration of reactants upon stepwise addition-removal of NH_3 in the SCR of NO at 473 K with 5 wt% vanadium fresh catalyst: (▲) NH_3, (■) NO, (●) N_2. Reacting gas composition: [NO] = 500 ppm, 3% O_2, [NH_3] = 600 ppm (when added), Ar to balance, total flow rate = 100 ml/min and GHSV = 34,000 h^{-1}.

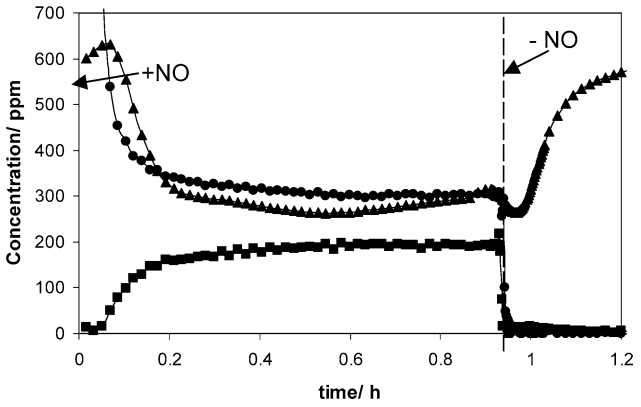

Fig. 7. Concentration of reactants upon stepwise addition-removal of NO in the SCR of NO at 423 K with 5 wt% vanadium sulphated catalyst: (▲) NH_3, (■) NO, (●) N_2. Reacting gas composition: [NH_3] = 600 ppm, 3% O_2, [NO] = 500 ppm (when added), Ar to balance, total flow rate = 100 ml/min and GHSV = 34,000 h^{-1}.

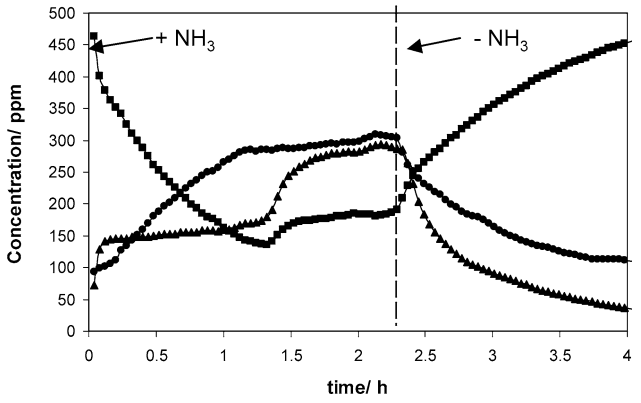

Fig. 8. Concentration of reactants upon stepwise addition-removal of NH_3 in the SCR of NO at 423 K with 5 wt% vanadium sulphated catalyst: (▲) NH_3, (■) NO, (●) N_2. Reacting gas composition: [NO] = 500 ppm, 3% O_2, [NH_3] = 600 ppm (when added), Ar to balance, total flow rate = 100 ml/min and GHSV = 34,000 h^{-1}.

tionary values that are negligible for temperatures lower than 500 K.

If we look at the CO_2 desorbed in TPReaction in the absence of O_2 (curves c and d), no gasification of labile carbon groups of support occurs in these experiments, for the fresh or sulphated catalyst. This reveals that lattice oxygen from sulphated catalyst is not able to oxidise the most labile carbon groups of support, but, as already mentioned, it can readily reoxidise vanadium.

3.4. Characterisation by transient-response techniques

Figs. 5 and 6 show experiments with stepwise addition-removal of NO and NH_3, respectively, to the fresh catalyst at 473 K. In Fig. 5, upon the introduction of NO, initially there is a high NO consumption, and, in parallel, the concentrations of N_2 and NH_3 rise. This takes place because of the high initial NH_3 coverage of the surface. Subsequently, NO concentration stabilises to the stationary values. Upon NO shutoff, the concentrations of NO and N_2 drop sharply, suggesting that NO reacts from gas phase or from a weakly adsorbed state. In Fig. 6, upon NH_3 shutoff, the concentrations of NO, N_2 and NH_3 do not reach the steady state instantaneously, but after 24 min. This suggests that NH_3 reacts from a strongly adsorbed state. The concentration of NO starts to rise as soon as NH_3 is shut-off, with a corresponding decrease in N_2 concentration. This indicates that the SCR reaction rate depends on the NH_3 coverage in the fresh catalyst.

Figs. 7 and 8 show the experiments with stepwise addition-removal of NO and NH_3, respectively, to the presulphated catalyst at 423 K. This temperature has been chosen deliberately to be lower than in the case of the fresh catalyst because at 473 K the conversion in the sulphated catalyst is complete, and, consequently, no variation upon NO addition is observed. The behaviour of the gas concentrations in experiments with stepwise addition-removal of NO (Fig. 7) is comparable to that in the fresh catalyst (Fig. 5). Accordingly,

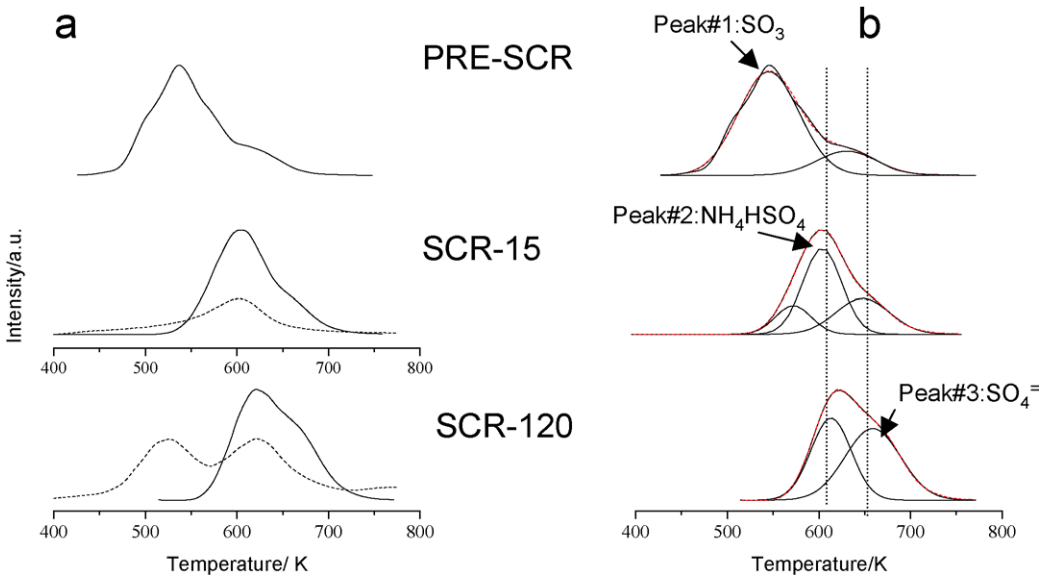

Fig. 9. TPD up to 773 K of sulphated 5 wt% vanadium catalyst after different stages of reaction: (PRE-SCR) just after the presulphation process; (SCR-15) after 15 min time-on-stream of the SCR reaction at 423 K, i.e. within the induction period; (SCR-120) after 120 min time-on-stream of the SCR reaction at 423 K, i.e. at steady state. (a) (—) SO_2 desorption, (- - - -) NH_3 desorption. (b) Deconvolution of SO_2 desorption peaks.

NO reacts from gas phase or a weakly adsorbed state both in fresh and presulphated catalyst. Upon NH_3 admission in the sulphated catalyst (Fig. 8) there is an induction period of around 90 min before the steady-state conversion is reached. In this time a large amount of NH_3 is consumed, and the curve of NH_3 exhibits a breakthrough just before the steady state is reached. From this, it is obvious that the building up of some ammonium sulphate species is needed to reach the enhanced conversion at steady state of the sulphated catalyst. The buildup of this ammonium sulphate species is a slow process. This large induction period was not observed for the second use of the catalyst, suggesting that once the sulphate species are formed, they remain on the catalyst. Upon NH_3 removal the reaction still proceeds to some extent for more than 90 min. This period is much longer than the 24 min that it takes the fresh catalyst to finish the reaction upon NH_3 removal. The reason for this can be found in the larger reservoir of adsorbed NH_3 in the sulphated catalyst. Integration of the area above the NO curve after NH_3 shutoff gives an indication of the reacted NO and therefore of the NH_3 stored in the catalyst. Simple calculations show that reacted NO is 0.34 ml in the fresh catalyst and 1.4 ml in the sulphated one. Furthermore, in the latter catalyst the reaction is far from finished. In a previous work [18], NH_3-TPD experiments showed that the sulphated catalyst is able to adsorb about two orders of magnitude more NH_3 than the fresh one. Despite the large NH_3 reservoir, it is apparent that the SCR reaction rate decreases; that is, N_2 concentration diminishes and NO concentration increases, as soon as NH_3 is removed from the feed gas. This suggests that the main storage of NH_3 takes place in sites different from active sites.

Table 1
Results of the deconvolution of SO_2 desorption profiles

Catalyst	Desorption peaks	Temperature (K)	Area	Percentage of total area (%)
PRE-SCR	Peak 1	536	4.26	81
	Peak 2	615	0.97	19
	Peak 3	–	0	0
SCR-15	Peak 1	565	0.47	7.7
	Peak 2	601	4	66
	Peak 3	651	1.6	26.3
SCR-120	Peak 1	–	0	0
	Peak 2	613	2.1	45.3
	Peak 3	658	2.5	54.7

3.5. Characterisation by temperature-programmed desorption

TPD was carried out to characterise the sulphate species involved in the SCR reaction of presulphated catalyst. The catalyst with 5% V was characterised by TPD just after the sulphatation process (PRE-SCR), after 15 min of the SCR reaction on stream at 423 K (SCR-15) (i.e., within the induction period) and after 120 min of the SCR reaction on stream at 423 K (SCR-120) (i.e., after steady state is reached). Fig. 9a shows the TPD-desorption profiles of SO_2 and NH_3, and Fig. 9b shows the deconvolution of the SO_2 profile. Table 1 displays the parameters of the deconvolution. The NH_3 and SO_2 profiles of the catalyst in the different stages show substantial differences. The temperature at which SO_2 starts to be released is 465, 524, and 551 K for the PRE-SCR, SCR-15, and SCR-120 catalysts, respectively. It is obvious that the stability of the sulphates increases during the SCR induction period. As derived from the previous section, the

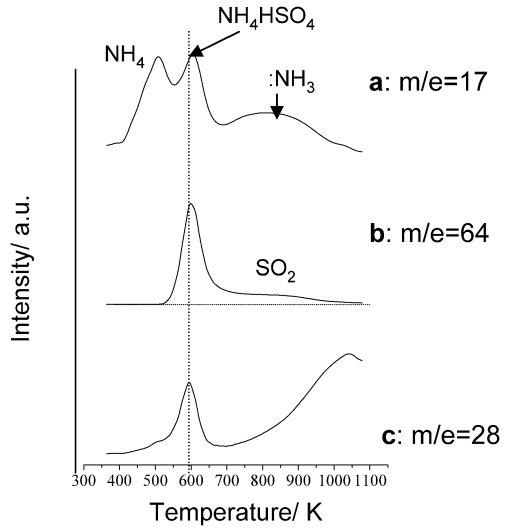

Fig. 10. TPD desorption profile after NH_3 preadsorption at 373 K with sulphated 5% V catalyst after steady state SCR reaction at 423 K during 72 h. Reacting gas composition: 500 ppm NO, 600 ppm NH_3, 3% O_2, 400 ppm SO_2 and Ar to balance. Total flow rate = 100 ml/min and GHSV = 34,000 h^{-1}. Spectrometer signals: (a) $m/e = 17$, (b) $m/e = 64$, (c) $m/e = 28$.

buildup of ammonium sulphates is an intermediate step for the formation of these more stable sulphate species. Concerning the NH_3 desorption profile, the SCR-15 catalyst only exhibits a peak at 602 K, associated with sulphate decomposition, whereas SCR-120 shows two peaks, one at 521 K for adsorbed NH_3 and a second peak at 621 K coinciding with a desorption of SO_2. The appearance of the NH_3 adsorption peak at 521 K suggests an increase in acid sites different from ammonium sulphates.

In the deconvolution of the SO_2 profile (Fig. 9b), three peaks can be distinguished: a low-temperature peak centred between 536 and 565 K (peak 1), one middle-temperature peak centred in the 601–615 K range (peak 2), and a high-temperature peak centred in the 651–658 K range (peak 3). In catalyst PRE-SCR, peak 1 is predominant, with 81% of total SO_2 released. In SO_2-TPD of SCR-15 catalyst, peak 1 has decreased drastically, and the intensities of peak 2 and peak 3 are larger than those in PRE-SCR, with peak 2 predominating over peak 3. In SO_2-TPD of SCR-120, peak 1 has fully vanished, the area of peak 2 has decreased, and that of peak 3 has increased. Thus the intensity of peak 1 decreases during the SCR induction period and almost disappears after 15 min on stream. This brings about an increase in peak 2, and, when SCR proceeds further, peak 2 partially transforms in more stable species (peak 3).

We also carried out TPD of preadsorbed ammonia up to 1073 K on fresh and sulphated catalyst after SCR reaction at 423 K for 72 h in the presence of SO_2. The gas composition in SCR experiments was 500 ppm NO, 600 ppm NH_3, 3% O_2, 400 ppm SO_2, and Ar as the balance. The catalyst has not shown any significant deactivation in these experiments, which emphasises the stability of the catalyst, even in the presence of a significant amount of SO_2 in the feed.

Fig. 10 shows the NH_3-TPD desorption profiles of $m/e = 17$ (NH_3), $m/e = 64$ (SO_2), and $m/e = 28$ (N_2 or CO) for the presulphated catalyst after SCR reaction. The integration of the NH_3 profile showed that the sulphated catalyst adsorbs two orders of magnitude more NH_3 than does the fresh catalyst [18]. The latter (not shown here) only showed a NH_3 desorption at 500 K (weakly bound NH_3) but did not exhibit desorption of NH_3 at temperatures higher than 600 K. On the other hand, the sulphated catalyst (Fig. 10) showed a NH_3 desorption at 500 K (weakly bound NH_3) and at 605 K (forming ammonium sulphates) and a broad peak from 700 to 1000 K (strongly bound NH_3). The SO_2 desorption ($m/e = 64$) shows the peak at 605 K, due to ammonium sulphates, and a shallow shoulder from 700 to 1000 K for very stable sulphates. The profile of $m/e = 28$ indicates that upon sulphate decomposition there is an ensuing gasification of carbon support (CO), but this signal may also include N_2 produced by oxidation of strongly bound ammonia.

3.6. Characterisation of catalysts by XPS

XPS spectra were recorded for the fresh and sulphated catalyst (Fig. 11). Binding energies (eV) and surface atomic ratios are listed in Table 2. The binding energy of V 2p is 517.0 and 517.2 in the fresh and sulphated catalysts, respectively. These binding energies indicate that vanadium is in oxidation state 5+ in both catalysts. There is a small shift (+0.2 eV) to higher binding energies in the sulphated catalyst with respect to the fresh one. This shift is only slightly higher than the uncertainty of the measure (0.1 eV), and it can be considered to be caused by the presence of an electronegative group as sulphates in the vicinity of V^{5+}. The binding energy of the S 2p peak at 168.7 eV is typical of sulphur in oxidation state 6+ as sulphates. The C 1s peak can be deconvoluted in two components: a first intense one at 284.9 eV, due to C–C bonds in aromatic and/or aliphatic structures, and a weak one at 286.3 eV due to single C–O bonds. This latter carbon species may account for the labile carbon atoms evolved in the initial stages of SCR.

The V/C ratio (Table 2) decreases upon sulphation, suggesting a certain agglomeration of VO_x units. The low surface density of vanadium (5 VO_x per 1000 carbon) and the higher surface density of sulphates (16 S per 1000 carbon) shows that sulphate species are mostly anchored to carbon.

XPS spectra were recorded for the sulphated catalyst after SCR reaction at 423 K for 72 h. The XPS spectra of N 1s shows two peaks, one at 399.4 eV with a 40% relative abundance and the other at 401.2 eV with a 60% relative abundance. The peak at 401.2 eV can be ascribed to ammonium ion because its value is close to the values reported in the literature for ammonium salts. For instance, the binding energies of N 1s core-level in NH_4Cl and NH_4NO_3 are 401.7 and 401.9 eV, respectively [9]. This ammonium ion can either form the sulphate salt or be chemisorbed on Brønsted acid sites. From the relative abundances of each

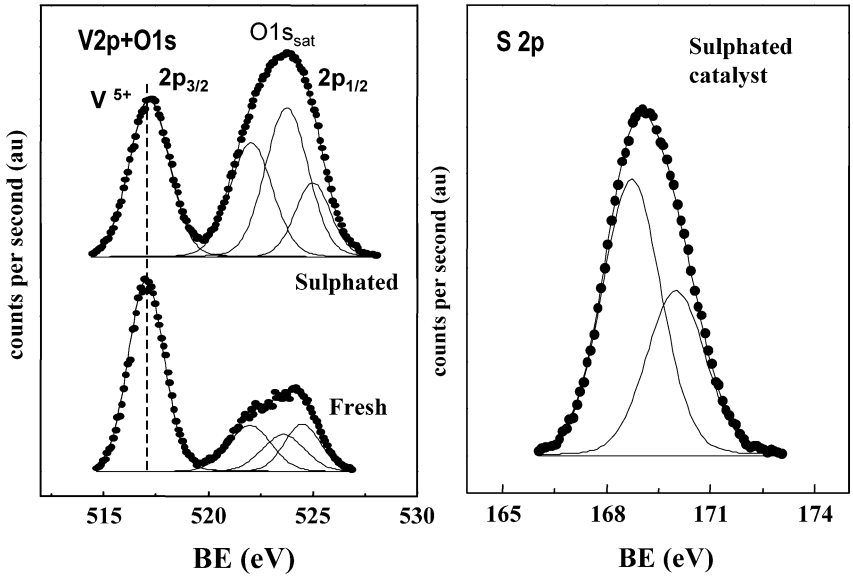

Fig. 11. XPS spectra: at the left, spectra of V 2p in fresh and sulphated catalyst; at the right, spectra of S 2p of sulphated catalyst.

Table 2
Binding energies (eV) and surface atomic ratios of 5 wt% V oxide on carbon coated monolith catalyst fresh and presulphated before and after SCR reaction at 423 K during 72 h[a]

Catalyst	C 1s	V 2p	S 2p	V/C atom	S/V atom	N 1s (relative abundance)
Fresh	284.9 286.3	517.0	–	0.010	–	–
Sulphated	284.9 286.3	517.2	168.7	0.005	3.20	–
Sulphated after SCR	284.9 286.3	517.2	168.7	0.006	4.2	399.4 (40) 401.2 (60)

[a] Reacting gas composition: 500 ppm NO, 600 ppm NH_3, 3% O_2, 400 ppm SO_2 and Ar to balance.

peak, it is apparent that ammonia is predominantly present as ammonium ion, since a great part of ammonia is forming ammonia sulphate salts, as deduced from NH_3-TPD. On the other hand, the peak at 399.2 eV can be assigned to ammonia molecularly chemisorbed on Lewis acid sites. This binding energy is higher than that of free NH_3 (a Lewis base), which is 398.9 eV. Electron donation from the lone pair of electrons of the N atom of the NH_3 molecule to the Lewis-acid site leads to a higher binding energy than that of free NH_3.

4. Discussion

From a comparison of experiments on stepwise addition-removal of NH_3 (Fig. 8) with SO_2-TPD experiments (Fig. 9) in the sulphated catalyst, it is apparent that sulphate species endowed with higher stability are developed during the induction period observed in the former experiment. In the SO_2-TPD profile, peak 2 can be unambiguously assigned to ammonium sulphates because it coincides with the desorption of ammonia. Peak 1 is the most abundant species in catalyst PRE-SCR, and it can be ascribed to sulphur oxides less stable than sulphates, most likely adsorbed SO_3. This adsorbed SO_3 becomes $SO_4^=$ as the SCR proceeds because of reaction of SO_3 with water produced in the SCR. This process is relatively fast, since after 15 min of SCR reaction more than 89% of SO_3 (peak 1) has been transformed to $SO_4^=$ (peak 2). As the SCR reaction proceeds further, the increase in peak 3 is apparent. This is a slower process, which takes around 90 min, and at steady state these very stable sulphate species (peak 3) are predominant over the less stable ammonium sulphates (peak 2).

The most stable sulphate species (peak 3 in SO_2-TPD) formed during the induction period is not associated with NH_3. Hence they are not forming ammonium sulphates and should be responsible for the superior performance of sulphated catalyst compared with the fresh one. Some evidence has been produced by this work that enables us to associate these species with sulphates neighbouring vanadium sites. The superior activity of the sulphated catalyst can be explained because these sulphates facilitate the reoxidation of vanadium, thus improving the redox properties, as proved by TPReaction experiments in the absence of O_2 (Fig. 3). In these experiments, the SCR reaction proceeds to a considerable degree in the absence of O_2 for the sulphated catalyst but not for the fresh one. Hence, lattice oxygen from sulphates close to vanadium is involved in the reoxidation of the catalyst. Despite the enhanced mobility of lattice oxygen for reoxidation of vanadium in the sulphated catalyst, this catalyst does not exhibit evolution of CO_2 in the absence of gas-phase O_2 (curve c, Fig. 4). Therefore this lattice oxygen does not contribute to gasification of the most labile carbon groups. The ability of these sulphate species to reoxidise vanadium and hence promote the SCR reaction, along with the inability to oxidise the most labile carbon groups from support is clear evidence for the assignment of these

species to sulphates in the vicinity of vanadium groups. The positive shift in V 2p binding energy (Fig. 11, Table 2) in the sulphated catalyst also supports the occurrence of an interaction between sulphates and vanadium sites. Hence sulphates must be close to vanadium sites. In forthcoming research, we intend to use Raman spectroscopy to identify possible structural changes in vanadyl sites induced by sulphates.

Several authors described the adsorption of sulphates on catalysts that are not supported on carbon but on metal oxides [12,13,27,28]. The promoting effect of sulphates on the catalytic activity of SCR at high temperature (> 523 K) has been attributed to the enhanced chemisorption of ammonia [9,12,13]. Sulphates are new acid sites on which NH_3 is adsorbed. The increase in acid sites in our sulphated catalyst is apparent from the increase in the NH_3 desorption peak at 521 K during the induction period (Fig. 9a). The increase in acid strength due to sulphates is also described in the literature [13,29]. S=O has a covalent double bond and has a much stronger affinity for electrons as compared with that of simple metal. Hence the Lewis acid strength of vanadium becomes substantially stronger because of the inductive effect of S=O. The presence of Lewis acid sites in relatively high amounts (40%) was confirmed by XPS results. When a water molecule is bonded to the Lewis acid site, the Lewis acid site can become a Brønsted acid site. The increase in acid strength created by the inductive effect of the S=O bond is demonstrated in our catalyst by the positive shift of V 2p binding energy and by the broad NH_3 peak between 700 and 1000 K in NH_3-TPD of sulphated catalyst after the SCR reaction (Fig. 10). This desorption of strongly bound NH_3 is not correlated with an equivalent SO_2 desorption at temperatures higher than 700 K. Thus NH_3 must be strongly bound to vanadium sites with a high acid strength due to the inductive effect of the S=O bond. This also confirms the fact that some sulphate groups are in the vicinity of vanadium because the inductive effect may occur in vanadyl groups relatively close to sulphates because of the extension of the charge delocalisation to the support [30].

As we have observed in NH_3 stepwise addition-removal experiments with fresh (Fig. 6) and sulphated (Fig. 8) catalysts, NH_3 reacts from an adsorbed state. Unlike the results reported in the literature for V_2O_5–WO_3/TiO_2 [11,21,22], in our catalyst the SCR reaction rate decreases immediately after NH_3 shutoff in both the fresh and sulphated catalysts. This occurs despite the large NH_3 reservoir of sulphated catalyst. Accordingly, the higher ammonia surface content in sulphated catalyst cannot account for the enhanced SCR activity at steady state. This decrease in SCR reaction rate upon NH_3 shutoff can be explained because the storing and activating sites of ammonia are different, and the process of NH_3 desorption from storing sites (i.e., as ammonium sulphates on carbon) and readsorption on vanadium active sites is a relatively slow process at these low reaction temperatures. In contrast, we postulate that the enhanced conversion in sulphated catalyst at steady state is due to the superior redox properties of this catalyst. Other research has found evidence that the reoxidation of V^{4+} may be rate limiting at low temperatures [21,31–33]. Our experimental results also support the conclusion that the reactivity is controlled by the reoxidation of V^{4+}, that is, by the mobility of lattice oxygen, rather than by the amount of adsorbed ammonia. To the best of our knowledge, this enhancement of the redox properties by surface sulphates is not described in the literature.

5. Conclusions

According to transient-response experiments, the SCR reaction of NO at low temperatures (393–523 K) over vanadium supported on carbon-coated monoliths, both fresh and presulphated, takes place between strongly bound ammonia and gaseous or weakly bound NO, in line with an Eley–Rideal mechanism. In SCR isothermal tests, presulphated catalyst exhibits almost twofold higher conversion at steady state than fresh catalyst. The former shows complete conversion and 100% selectivity for N_2 at a temperature of 473 K. One difference between fresh and presulphated catalyst is that the presulphated catalyst is able to store about two orders of magnitude more ammonia compared with the fresh catalyst. The higher amount of stored ammonia cannot account for the higher SCR activity at steady state. This reveals that the storing and activating sites of ammonia are different in the sulphated catalyst. In contrast to fresh catalyst, sulphated catalyst showed relevant activity in the absence of gas-phase O_2. Thus sulphated catalyst has superior mobility of lattice oxygen, which is involved in the reoxidation of vanadium during the redox process.

With the presulphated catalyst, a slow induction period occurs in the SCR reaction before steady state is reached. In this induction period, more stable sulphate species are developed, as suggested by SO_2-TPD. These very stable sulphates must account for the enhanced conversion. These sulphate groups are located in the vicinity of vanadyl groups, since they facilitate the reoxidation of vanadium during the SCR in the absence of gas-phase O_2. Furthermore, these sulphate groups do not contribute to the gasification of the most labile carbon groups of support. Another additional feature of the sulphate species is the increase in acid strength of vanadium sites due to the inductive effect of the S=O bond. This fact also confirms that these sulphate structures are in close proximity to vanadium sites. To summarize: the superior SCR activity at low temperatures of sulphated catalyst compared with fresh catalyst can be ascribed to the close interaction of vanadium and sulphates. This interaction enhances the reoxidation of reduced vanadium by lattice oxygen from sulphates neighboring vanadium sites.

Acknowledgments

The authors thank Hüttenes-Albertus, Hannover (Germany), for supplying the furan resin. The authors are in-

debted to the Spanish Ministry of Science and Technology (PPQ-2002-02698) and the "Diputacion General de Aragón" for financial support. E.G.-B. acknowledges the MCyT for a "Ramón y Cajal" contract.

References

[1] L. Singoredjo, R. Korver, F. Kapteijn, J. Moulijn, Appl. Catal. B: Environ. 1 (1992) 297.
[2] P. Smirniotis, D. Peña, B. Uphade, Angew. Chem. Int. Ed. 40 (2001) 2479.
[3] M. Richter, A. Trunschke, U. Bentrup, K. Brzezinka, E. Schreier, M. Schneider, M. Pohl, R. Fricke, J. Catal. 206 (2002) 98.
[4] T. Valdes-Solis, G. Marbán, A.B. Fuertes, Appl. Catal. B: Environ. 46 (2003) 261.
[5] Z. Zhu, Z. Liu, H. Niu, S. Liu, J. Catal. 187 (1999) 245.
[6] G. Marbán, T. Valdes-Solis, A.B. Fuertes, Phys. Chem. Chem. Phys. 6 (2004) 453.
[7] T. Grzybek, J. Pasel, H. Papp, Phys. Chem. Chem. Phys. 1 (1999) 341.
[8] R. Long, R. Yang, R. Chang, Chem. Commun. (2002) 452.
[9] J. Chen, R. Yang, J. Catal. 139 (1993) 277.
[10] P. Ciambelli, M.E. Fortuna, D. Sannino, A. Baldacci, Catal. Today 29 (1996) 161.
[11] L. Lietti, G. Ramis, F. Berti, G.P. Toledo, D. Robba, G. Busca, P. Forzatti, Catal. Today 42 (1998) 101.
[12] R.Q. Long, M. Chang, R. Yang, Appl. Catal. B: Environ. 33 (2001) 97.
[13] R.Q. Long, R.T. Yang, J. Catal. 186 (1999) 254.
[14] S. Jung, P. Grange, Appl. Catal. B: Environ. 32 (2001) 123.
[15] M. Amiridis, I. Wachs, G. Deo, J. Jehng, D. Kim, J. Catal. 161 (1996) 247.
[16] Z. Zhu, Z. Liu, S. Liu, H. Niu, Appl. Catal. B: Environ. 23 (1999) 229–233.
[17] Z. Zhu, Z. Liou, H. Niu, S. Liu, T. Hu, T. Liu, Y. Xie, J. Catal. 197 (2001) 6.
[18] E. Garcia-Bordeje, A. Monzón, M.J. Lázaro, R. Moliner, Catal. Today (2005), in press.
[19] E. Garcia-Bordeje, M.J. Lazaro, R. Moliner, J.F. Galindo, J. Sotres, A.M. Baro, J. Catal. 223 (2004) 395.
[20] Z. Zhu, H. Niu, Z. Liu, S. Liu, J. Catal. 195 (2000) 268.
[21] L. Lietti, I. Nova, S. Camurri, E. Tronconi, P. Forzatti, AIChE J. 43 (1997) 2559.
[22] E. Tronconi, L. Lietti, P. Forzatti, S. Malloggi, Chem. Eng. Sci. 51 (1996) 2965.
[23] J. Dunn, P. Koppula, H. Stenger, I. Wachs, Appl. Catal. B: Environ. 19 (1998) 103.
[24] E. Tronconi, A.O.C. Cavanna, P. Forzatti, Ind. Eng. Chem. Res. 38 (1999) 2593.
[25] J. Svachula, L. Alemany, N. Ferlazzo, P. Forzatti, E. Tronconi, Ind. Eng. Chem. Res. 32 (1993) 826.
[26] G. Centi, N. Passarini, S. Perathoner, A. Riva, Ind. Eng. Chem. Res. 31 (1992) 1947.
[27] O. Saur, M. Bensitel, A.B. Mohammed Saas, J.C. Lavalley, C.P. Tripp, B.A. Morrow, J. Catal. 99 (1986) 104.
[28] T. Jin, T. Yamaguchi, K. Tanabe, J. Phys. Chem. 90 (1986) 4794.
[29] J. Chen, R. Yang, J. Catal. 125 (1990) 411.
[30] J. Bernholc, J.A. Horsley, L.L. Murrel, L.G. Sherman, S. Soled, J. Phys. Chem. 91 (1987) 1526.
[31] L. Alemany, L. Lietti, N. Ferlazzo, P. Forzatti, G. Busca, E. Giamello, F. Bregani, J. Catal. 155 (1995) 117.
[32] L. Casagrande, L. Lietti, I. Nova, P. Forzatti, A. Baiker, Appl. Catal. B: Environ. 22 (1999) 63.
[33] M. Koebel, G. Madia, F. Raimondi, A. Wokaun, J. Catal. 209 (2002) 159.